

# Geometry and scaling of cosmic voids

José Gaité

Instituto de Microgravedad IDR, ETS Ingenieros Aeronáuticos, Universidad Politécnica de Madrid, E-28040 Madrid, Spain;  
jose.gaité@upm.es

October 26, 2018

## ABSTRACT

*Context.* Cosmic voids are observed in the distribution of galaxies and, to some extent, in the dark matter distribution. If these distributions have fractal geometry, it must be reflected in the geometry of voids; in particular, we expect scaling sizes of voids. However, this scaling is not well demonstrated in galaxy surveys yet.

*Aims.* Our objective is to understand the geometry of cosmic voids and its relation to the geometry of the galaxy and dark-matter distributions. We examine the consequences of a fractal structure of matter and, in particular, the hypothesis of scaling of voids. We intend to distinguish monofractal voids from multifractal voids, regarding their scaling properties. We plan to analyse voids in the distributions of mass concentrations (halos) in a multifractal and their relation to galaxy voids.

*Methods.* We begin with a statistical analysis of point distributions based on the void probability function and correlation functions. An analytical treatment is possible if we assume that voids are spherical. Therefore, we devise a simple spherical void finder. For continuous mass distributions, we employ the methods of fractal geometry. These methods provide analytical predictions, which we confirm with numerical simulations. Smoothed mass distributions are suitable for the method of excursion sets.

*Results.* Voids are very nonlinear and non-perturbative structures. If the matter distribution has fractal geometry, voids reflect it, but not always directly: scaling sizes of voids imply fractal geometry, but fractal voids may have a complicated geometry and may not have scaling sizes. Proper multifractal voids are of this type. A natural multifractal biasing model implies that the voids in the galaxy distribution inherit the same complicated geometry.

*Conclusions.* Current galaxy surveys as well as cosmological  $N$ -body simulations indicate that cosmic voids are proper multifractal voids. This implies the presence in the voids of galaxies or, at least, small dark matter halos.

**Key words.** cosmology: large-scale structure of Universe – galaxies: clusters:general – methods: statistical

## 1. Introduction

The large scale structure of matter is formed by clusters, filaments, sheets, and voids. The rôle of voids as basic ingredients of the large scale structure is now well established, but the definition of what constitutes a void is still imprecise. Originally, voids were described as large regions devoid of galaxies, but the current view is more complex (Peebles, 2001). Consequently, the theory has developed progressively to consider more sophisticated models of voids. Nowadays, there is a good amount of statistics of galaxy voids, and there is also information about voids as a part of the more general information about cosmic structure that is obtained in  $N$ -body simulations of cold dark matter (CDM). It seems that it should be possible to determine the main features of voids by combining observational data with theoretical models.

Here, we are interested in the features of voids related to the scale invariance and fractal geometry of the cosmic structure. Scale invariance is a general symmetry, which can manifest itself in physical systems in various ways. In cosmology, it gave rise to hierarchical models of the Universe, related to fractal geometry (Mandelbrot, 1983). Some evidence for them was provided by the analysis of galaxy catalogues, which found that the two-point correlation function is a power law on scales of several Mpc, and found, with less confidence, that higher-order correlation functions are also power laws (Peebles, 1980). Self-similar fractal models of the galaxy distribution have been well studied (Pietronero, 1987; Sylos Labini, Montuori & Pietronero, 1998); also, multifractal models (Jones et al, 1988; Balian & Schaeffer,

1988; Martínez, Jones, Domínguez-Tenreiro & van de Weygaert, 1990). Recent reviews of various ideas and models in cosmology based on scaling laws are given by Jones et al (2004) and by Gabrielli et al (2005).

Mandelbrot (1983) introduced the notion of fractal holes (“tremas”) and considered its application to the galaxy distribution. In fact, he was concerned with the absence of large voids in this distribution and introduced the concept of lacunarity in this regard: two fractals with equal dimension can differ in their lacunarity, in such a way that the less lacunar one appears as if it had larger dimension (roughly speaking, as if it were less fractal). Besides, Mandelbrot (1983) characterized some fractals as having a power-law distribution of void sizes.

Regarding astronomical measures of voids, self-similarity of voids was already considered by Einasto et al (1989) as a probe of scale invariance in the large scale structure. Following Mandelbrot (1983), we proposed that a manifestation of the self-similarity of voids, as it appears in fractal distributions, is that the rank-ordering of their sizes fulfills Zipf’s power law (Gaité & Manrubia, 2002). In particular, the transition from this power law to a different dependence at small ranks, namely, the fact that the largest voids have almost constant size, marks the transition to homogeneity on very large scales (Gaité, 2005-B). Thus far, the scaling of galaxy void sizes remains moot. Our early analysis of void catalogues did not show any evidence of a Zipf law (Gaité & Manrubia, 2002), but analyses of recent surveys are more favourable (Tikhonov & Karachentsev, 2006; Tikhonov,

2006; Tikhonov, 2007). However, scaling over a convincingly large range has not been demonstrated yet.

Otto et al. (1986) regarded the significance of cosmic voids, namely, they regarded whether voids were really elements of the large scale structure or just the necessary fluctuations about homogeneity. They developed statistical methods to answer this question. These methods were improved and generalized by Betancort-Rijo (1990). Our statistical methods are based on theirs, but our constructions are addressed to the study of the nonlinear regime and, in particular, the analysis of its scale invariant features.

The detection of voids in galaxy samples is carried out with computer algorithms called void-finders. These algorithms have evolved in accord with the observational and theoretical ideas about voids, in particular, in accord with the ideas about their emptiness. Initially, voids were defined as empty spheres of maximal radii (Einasto et al, 1989). Later, more general shapes were allowed, and voids were also allowed to contain some galaxies, as in, e.g., the popular void-finder devised by El-Ad & Piran (1997), which separates “field galaxies” from “wall galaxies.” We have defined an algorithm for finding voids of arbitrary shape based on discrete-geometry constructions (Gaité, 2005-B). Here, we return to the old spherical voids, which are more adequate for the application of analytical methods. In particular, they are adequate for designing a parameter-free void-finder. Spherical voids are also favoured by theoretical arguments (Icke, 1984).

There is no substantial observational knowledge of the geometry of voids in the dark matter distribution. Notwithstanding, voids have been studied in cosmological  $N$ -body simulations of CDM models. Gottlöber et al (2003) have re-simulated voids with higher resolution and found structures inside them, in a self-similar pattern. Recently, Sheth & van de Weygaert (2004) and Shandarin, Sheth & Sahni (2004) have defined voids as *underdense connected* regions, such that they are complementary to clusters. With this definition, voids contain matter and have very complex shapes.

The hypothesis of scale invariance in the nonlinear regime leads to a self-similar multifractal model of the dark matter distribution, which is supported by the analysis of cosmological simulations (Gaité, 2005-A, 2007). It is natural to define voids in a multifractal as locations of mass depletions (Gaité, 2007). We study here the geometry of these voids, which is very complicated, even more complicated than the geometry of the voids in the models of Sheth & van de Weygaert (2004) or Shandarin, Sheth & Sahni (2004). Assuming that the dark-matter distribution is multifractal, it is desirable to relate multifractal voids, which have complex shapes and may contain matter, to simpler definitions applicable to galaxy voids (which are the ones that we can directly observe). Two questions are important in this regard: (i) the role of the small number density the distribution of galaxies in comparison with the distribution of dark matter, which can be considered continuous; (ii) the statistical relation of the distribution of galaxies to the distribution of dark matter, which can be direct or involve galaxy biasing.

Regarding the number density of galaxies, we study how the nature of voids in a sample of a continuous distribution changes with the density of the sampling, especially, in the nonlinear regime. Regarding galaxy biasing, we only consider a simple model, which relies on the “peak theory” of Gaussian fields (Kaiser, 1984; Bardeen et al, 1986). However, we introduce the non-Gaussian character of the density field in the nonlinear regime by substituting Gaussian peaks by nonlinear mass concentrations (halos), as proposed before (Gaité, 2005-A, 2007).

Therefore, we can apply our results about scaling in the distribution of halos of given mass in a multifractal cosmic distribution.

We begin with a brief review of the notion of a void in a discrete mass distribution. We call this type of voids Poissonian voids. Indeed, a complete analytical study of this type of voids can be carried out for a Poisson distribution (Sect. 2). This study is useful for setting up the analytical framework and for establishing the significance of voids. The generalization to correlated point distributions yields perturbative expressions in terms of correlation functions (Sect. 3). The study of Poissonian voids is simplified by the definition of a void as an *empty* spherical region enclosed by a set of four non-coplanar points. Relying on this definition and imposing the condition that the voids do not overlap, we devise a simple and efficient void-finder (Sect. 4). Then, we consider the scaling of voids in monofractal distributions (Sect. 5). We review the definition and properties of cut-out sets as cosmic foam models (Gaité, 2006) and generalize that notion. With this background, we undertake the general case of multifractal voids, which leads us to differentiate two types of voids, in connection with their geometry (Sect. 6). Then, we study galaxy voids and galaxy biasing (Sect. 7). Finally, we discuss our results (Sect. 8).

## 2. Poissonian analysis of galaxy voids

Voids arose as large regions in the distribution of galaxies containing no galaxies or many fewer than the mean expected number of galaxies. Of course, there are fluctuations even in a homogeneous distribution of galaxies. Therefore, it is necessary to quantify the fluctuations.

To be precise, a homogeneous Poisson field (or process) is defined as a random sample of a uniform distribution, such that the probability of having a point in a given region is proportional to its volume. If the density (or intensity) of the field is  $n$ , then the probability of having  $k$  points in a region of volume  $V$  is given by the familiar Poisson distribution with parameter  $N = nV$ :

$$P_k[V] = \frac{N^k}{k!} e^{-N}.$$

Politzer & Preskill (1986) studied the statistics of clusters and voids in a Poisson field. This study was used by Otto et al. (1986) to determine the significance of the then observed galaxy voids. Their conclusion is that those voids were consistent with a homogeneous distribution of galaxies or, at any rate, with a homogeneous distribution of rich clusters of galaxies.

Central to the arguments of Otto et al. (1986) is the calculation by Politzer & Preskill (1986) of the probability per unit volume of having a void of given (and simple) shape in a random sample of points with a uniform distribution. The probability that a *given* region contains no points or contains fewer than the expected number of points is provided by the Poisson distribution. However, the calculation of the probability of having a void of given size and shape at any place is a more difficult problem. Its solution can be obtained with a careful analysis of the Poisson field. Their analysis is involved and their formula for the probability of a void has a questionable normalization. Since this formula is important, we re-derive it (with its normalization) using a different method that is more straightforward. Then, we re-analyse the significance of voids, regarding the voids in some recent galaxy surveys and their statistics.

### 2.1. Probability of a spherical void in a homogeneous distribution

The simplest shape of a void is certainly the spherical shape. Politzer & Preskill (1986) obtained the following formula for the probability per unit volume of a spherical void:

$$\mathbb{P}_k[V] = \left( \frac{3\pi^2}{32} \right) \frac{(nV)^3}{V} P_k[V],$$

where  $k$  is the number of points in the void, assumed to be much smaller than the expected number, namely,  $k \ll nV$ .

The probability density  $\mathbb{P}_k[V]$  should be normalized, that is to say, its integral over  $V$  from zero to infinity should be one. However, the constant  $3\pi^2/32$  does not normalize it, as is easily checked. Since Politzer & Preskill's formula for  $\mathbb{P}_k[V]$  is only valid for  $V \gg k/n$ , it cannot be normalized. Nevertheless, that condition is certainly fulfilled for all  $V > 0$  if  $k = 0$ , which suggests that the probability of an empty void  $\mathbb{P}_0[V]$  should be valid for all  $V$ .

If we assume that Politzer & Preskill's formula holds for all  $V$ , then the constant  $3\pi^2/32$  must be replaced with  $1/((k+2)(k+1))$ . Note that, then, only  $\mathbb{P}_0[V]$  (totally empty voids) refers to voids over the entire range of  $V$ . Using a method simpler than the one of Politzer & Preskill, we can prove that, in fact,

$$\mathbb{P}_k[V] = \left( \frac{1}{(k+2)(k+1)} \right) \frac{(nV)^3}{V} P_k[V], \quad (1)$$

is correct and holds over the entire range of  $V$ .

#### 2.1.1. Calculation of the probability $\mathbb{P}_k[V]$

The calculation of  $\mathbb{P}_k[V]$  for spherical voids can be formulated as follows. A spherical void is defined by four non-coplanar points on its boundary, because a void can always be enlarged so as to touch four points. In addition a  $k$ -void is defined to have  $k$  points inside. Since the points are uncorrelated, the probability distribution for each point is constant and independent of the other points. Therefore, we can calculate  $\mathbb{P}_k[V]$  as the product of the probability of four points and the conditional probability of having  $k$  points inside the sphere of volume  $V$  defined by them,  $P_k[V]$ .

The probability of each of the four points is the product of its volume element and the density  $n$ . Thus, the only problem is to express the four-point volume element in terms of a set of variables that includes the volume of the sphere defined by the four points. If we denote the positions of the points by  $\{x_i\}_{i=1}^4$  and the position of the center of the sphere (their circumcenter) by  $x_c$ , then

$$d^3 x_1 d^3 x_2 d^3 x_3 d^3 x_4 = d^3 x_c V^2 dV f(\theta_1, \theta_2, \theta_3, \theta_4) d^2 \theta_1 d^2 \theta_2 d^2 \theta_3 d^2 \theta_4,$$

where  $V$  is the sphere's volume,  $\{\theta_i\}_{i=1}^4$  are the four sets of two angular coordinates over the sphere, and  $f$  is a function of these angular coordinates. This expression follows from translation invariance and dilation covariance only. The function  $f$  can be calculated, but we do not need it. We obtain formula (1), without normalization, by factoring out both the integral over the angles and  $n d^3 x_c$ . A straightforward integration over  $V$  gives the correct normalization constant  $1/((k+2)(k+1))$ .

Let us remark that formula (1) involves *no approximation* and is valid for all  $V$ . However, it refers to voids only if  $k \ll$

$nV$ . In the case of empty voids ( $k = 0$ ), then  $P_0[V]$  approaches unity in the limit  $V \rightarrow 0$ , but  $\mathbb{P}_0[V]$  is small due to the boundary factor (corresponding to the four points defining the void). In other words, the probability that a randomly chosen small ball be empty is large, but the probability that it constitute a void is small. In fact, the most probable void size is  $V = 2/n$ . We can also calculate other statistical quantities, for example, the average void size,  $\bar{V} = 3/n$ .

### 2.2. The significance of large voids

Otto et al. (1986) used Politzer & Preskill's formula to determine the significance of some large voids that had been found at the time. In particular, they chose a totally empty void in the distribution of Abell clusters (rich clusters), in which the expected number of these clusters was 10. Then, Politzer & Preskill's formula, with  $k = 0$  and  $nV = 10$ , yields  $\mathbb{P}_0[V] = 0.042/V$ . Multiplying it by the total volume, which corresponds to a sample of 70 clusters, they obtain that the expected number of voids of that size is 0.3. However, if we replace the constant  $3\pi^2/32 = 0.93$  with its correct value,  $1/2$ , then the expected number of voids is halved, so that the void in question becomes less probable.

On the other hand, the actual void was ellipsoidal. Thus, we should consider the largest spherical void inscribed in it, which is quite smaller and, therefore, more probable. Alternately, we could use the formula given by Otto et al. (1986) for ellipsoidal voids.<sup>1</sup> At any rate, their conclusion was that such a void was not improbable even in a random distribution of Abell clusters. This negative conclusion needs revision, anyway, regarding recent data. In particular, we shall briefly regard below data from the 2dF and SDSS galaxy surveys that show that large voids are, in fact, very significant. Of course, this is the commonly accepted conclusion nowadays.

Let us explain in more detail the use of Eq. (1) to determine the departure of a point distribution from randomness. Since we are interested in large voids, we can use the cumulative probability of having a void of size equal or larger than  $V$ :

$$\mathbb{P}_{>}[V] = \int_V^\infty \mathbb{P}_0[v] dv \approx \frac{(nV)^2}{2} e^{-nV},$$

for large voids ( $nV \gg 1$ ). Setting  $nV = 10$  (as Otto et al.),  $\mathbb{P}_{>} = 0.0023$ , which is a fairly small number. However, the expected number of voids of size larger than  $V$  is naturally proportional to the size of the sample. Thus, it is a number relatively close to one for a moderate sample of 70 points and, in fact, it becomes larger than one for a large enough sample. Nevertheless, in a large sample, the natural question is if there are other large voids and their respective sizes.

In other words, for a complete study of the significance of voids in a sample, one must determine the sizes of many voids, beginning with the largest one. This is the standard void-finding procedure. Suitable void-finding algorithms are employed in this task. If the void-finder looks for voids by just fitting the largest sphere, then this spherical void should be the most significant. Smaller voids found in the sample are usually constrained not to overlap any preceding void (or not to overlap more than a given fraction of any preceding void). We will analyse a void-finder of this type in Sect. 4. Once the full set of voids in a sample is

<sup>1</sup> In this case, Otto et al. do not give the normalization constant, which depends on the maximum accepted eccentricity. This constant can be obtained with our method.

available, one can study the distribution of their sizes. In recent surveys, we usually find that the largest voids are very significant, but we see below that the overall distribution of void sizes can be even more significant.

### 2.2.1. Voids in recent surveys

Tikhonov (2006, 2007) has studied and rank-ordered the voids in samples of the 2dF and SDSS surveys. In particular, he has chosen from the 2dF survey a volume limited sample (VLS) with 7219 galaxies, such that the volume per galaxy is  $513 \text{ Mpc}^3 h^{-3}$ . The largest void in it corresponds to a sphere with radius  $21.3 \text{ Mpc } h^{-1}$  and volume  $4.05 \cdot 10^4 \text{ Mpc}^3 h^{-3}$ . Thus, if the sample belonged to a uniform distribution, the expected number of sample galaxies in that sphere would be 78.9. Then, the expected number of voids of that size would be  $(1/2) 7219 \times 78.9^2 e^{-78.9} = 1.21 \cdot 10^{-27}$ , that is, absolutely negligible.

Furthermore, Tikhonov (2006) finds a number of voids with corresponding spheres that have slightly smaller radii. All these voids are undeniably significant. Indeed, Tikhonov (2006) uses a numerical comparison with a random sample to determine that the largest 110 voids, with sphere radius larger than  $9 \text{ Mpc } h^{-1}$ , are significant. His criterion is to measure significance by  $1 - N_{\text{random}}(r)/N_{\text{survey}}(r)$ , where  $N_{\text{survey}}(r)$  and  $N_{\text{random}}(r)$  are the number of voids with radii larger than  $r$ , respectively, in the sample and in a random point distribution with the same boundaries and mean density. That quantity must be non-vanishing for significant voids. The mean number of galaxies in a sphere with radius of  $9 \text{ Mpc } h^{-1}$  is six, and the expected number of larger void spheres in the sample is  $N_{\text{random}}(6) = 460$ .<sup>2</sup> However, note that Tikhonov's criterion is less stringent than Otto et al's, which requires  $N_{\text{random}}(r) \ll N_{\text{survey}}(r)$ . In other words, Otto et al's criterion neglects voids that are just somewhat larger than the voids in a random point distribution, because the probability of such voids in a random point distribution is not sufficiently small.

The very recent analysis of SDSS voids (Tikhonov, 2007) yields similar results, regarding the size of the largest voids and, indeed, the overall distribution. We reanalyse in Sect. 7 Tikhonov's VLS from the 2dF survey, regarding the statistical properties of the distribution of its voids, in particular, its scaling properties.

## 3. Voids in correlated point distributions

It is possible to extend the preceding methods to correlated point fields.<sup>3</sup> Given that the distribution of galaxies is very inhomogeneous on small scales, this extension is necessary. Otto et al. (1986) already considered the modification of their results when the points are correlated rather than totally random, and studied it in terms of the cluster expansion. Betancort-Rijo (1990) employed a different method, which is more adequate when the correlations are strong.

We consider again the probability  $P_k[V]$  of having  $k$  points in a region of volume  $V$ . For the Poisson distribution, its maximum is at  $k \approx nV$  (which is also the mean). Naturally, the presence of density fluctuations makes  $P_k[V]$  larger when  $k$  differs from  $nV$ ,

<sup>2</sup> The smaller number reported by Tikhonov (2006), namely, 110, is due to the non-overlap condition and to the fact that his voids are not spherical and, therefore, they are larger.

<sup>3</sup> The precise formulation of this generalization actually involves *two* stochastic processes: the point process and the random process that produces the continuous distribution. Thus, it is called doubly stochastic process or Cox process.

in particular, when  $k \ll nV$ . Actually, the basic quantity that we need is  $P_0[V]$  (the void probability function), because  $P_k[V]$  can be obtained from it (White, 1979) and, besides, we are going to restrict ourselves to empty spherical voids.

### 3.1. The void probability function and the probability of spherical voids

Otto et al. (1986) relied on the expression of the void probability function (VPF) in terms of correlations. This function is analogous to the grand-canonical partition function of a statistical particle system in which their velocities have been integrated over. Therefore, the VPF admits an expansion in terms of the correlations that is analogous to the cluster expansion in statistical mechanics (see White 1979, for the introduction of the VPF in cosmology, Balian & Schaeffer 1989, for a more detailed study, and Mekjian 2007, for the connection with statistical mechanics).

In analogy with the cluster expansion, if the correlation functions decay rapidly on large distances, the void probability function can be expressed as

$$P_0[V] = \exp \left[ \sum_{k=1}^{\infty} \frac{(-nV)^k}{k!} \bar{\xi}_k \right], \quad (2)$$

where  $\bar{\xi}_1 = 1$ , and, for  $k \geq 2$ ,

$$\bar{\xi}_k = \frac{1}{V^k} \int_V d^3x_1 \cdots d^3x_k \xi_k(x_1, \dots, x_k).$$

Note that Eq. (2) reduces to the Poisson form in the uncorrelated case, namely, when  $\bar{\xi}_k = 0$  for  $k \geq 2$ .

The cumulants  $\bar{\xi}_k$ ,  $k \geq 2$ , vanish in the limit  $V \rightarrow \infty$ . Furthermore, in this limit, the larger  $k$  is, the more rapidly they vanish. Thus, the first approximation is to consider that only  $\bar{\xi}_2$  is non-vanishing, that is to say, to consider a random sample of a Gaussian field. The Gaussian approximation is reasonable, for example, when  $\sigma = \bar{\xi}_2^{1/2} < 0.32$ , because the probability that the density be negative is then smaller than 0.1%. However, in the weakly-correlated regime with  $\sigma = 0.32$ , the correction factor given by Eq. (2) is large even for small  $nV$ . For example, when  $nV = 4$ , we have  $\exp[(nV\sigma)^2/2] = 2.3$ , and, when  $nV = 10$  (as in the example in Sect. 2.2),  $\exp[(nV\sigma)^2/2] = 167$ . Naturally, the presence of density fluctuations results in an increase of the void probability function, an increase that can be large.

Let us mention that Otto et al. (1986), using the analogy with the cluster expansion, interpret Eq. (2) as a renormalization of the number density, such that

$$n_c = n \left( 1 + \sum_{k=1}^{\infty} \frac{(-nV)^k}{(k+1)!} \bar{\xi}_{k+1} \right)$$

is the density of clusters. Therefore, the statistics of voids on the scales of transition to homogeneity in a correlated point distribution is similar to the statistics of voids in an uncorrelated distribution with a lower density. Within this interpretation, and in the Gaussian approximation with  $\sigma = 0.32$  and  $nV = 10$ , we have that  $n_c = n(1 - nV\sigma^2/2) = 0.49n$ . But  $n_c$  turns negative when  $nV > 19$  and becomes meaningless. Given that  $n_c < 0 \Rightarrow P_0[V] > 1$ , we should not trust the Gaussian approximation if  $\sigma$  and  $nV$  are not sufficiently small for having positive  $n_c$ , whether we interpret it as a renormalized number density or not.

In a particular case of strong correlations, namely, in fractal distributions, the transition to homogeneity in the statistics of voids has been studied by Gaité (2005-B). The argument proposed there is that a fractal consists of a hierarchy of clusters of clusters and, therefore, it is invariant under coarse graining up to the homogeneity scale. Over this scale, the largest coarse-grained particles (clusters) become uncorrelated and, correspondingly, the largest voids are like voids in a Poisson distribution of clusters. Simulations of fractals confirm this view (Gaité, 2005-B).

In the weakly nonlinear regime, an improvement over the Gaussian approximation is the lognormal model (Coles & Jones, 1991). Its void probability function is given by the probability of having a void volume  $V$  in a density  $\rho$  integrated over the density; namely,

$$P_0[V] = \frac{1}{\sigma \sqrt{2\pi}} \int_0^\infty \exp\left[-\frac{(\ln \rho - \mu)^2}{2\sigma^2} - nV\rho\right] \frac{d\rho}{\rho}, \quad (3)$$

where  $\mu = -\sigma^2/2$  if we assume that  $\langle \rho \rangle = 1$ . This function tends to the Gaussian VPF when  $\sigma \rightarrow 0$  (when the correlations become small). With  $\sigma = 0.32$  and  $nV = 10$ , it yields  $P_0[V] = 7.61 \cdot 10^{-4}$ , which is 17 times larger than the Poisson value (Sect. 2.2). This factor is to be compared with the factor given by the Gaussian approximation, namely, 167, which is clearly an overshoot. Thus, this comparison questions the validity of the Gaussian approximation well before  $n_c$  becomes negative.

Once we have studied the VPF, we can generalize the calculation of  $\mathbb{P}_0[V]$  in Sect. 2.1.1. Let us begin with the expression for the probability of having an empty sphere of volume  $V$  with four non-coplanar points on its boundary, namely, with the four-point function

$$\begin{aligned} dP_{1234} = n^4 d^3 x_1 \cdots d^3 x_4 & \left[ \bar{\xi}(x_1) \bar{\xi}(x_2) \bar{\xi}(x_3) \bar{\xi}(x_4) + \right. \\ & \bar{\xi}(x_1, x_2) \bar{\xi}(x_3) \bar{\xi}(x_4) + \cdots + \bar{\xi}(x_1) \bar{\xi}(x_2) \bar{\xi}(x_3, x_4) + \\ & \bar{\xi}(x_1, x_2) \bar{\xi}(x_3, x_4) + \cdots + \bar{\xi}(x_1, x_4) \bar{\xi}(x_2, x_3) + \\ & \bar{\xi}(x_1, x_2, x_3) \bar{\xi}(x_4) + \cdots + \bar{\xi}(x_1) \bar{\xi}(x_2, x_3, x_4) + \\ & \left. \bar{\xi}(x_1, \dots, x_4) \right] P_0[V], \quad (4) \end{aligned}$$

where

$$\begin{aligned} \bar{\xi}(x) &= 1 + \sum_{k=1}^{\infty} \frac{(-n)^k}{k!} \int_V d^3 y_1 \cdots d^3 y_k \xi_{k+1}(x, y_1, \dots, y_k), \\ \bar{\xi}(x_1, x_2) &= \xi_2(x_1, x_2) + \\ & \sum_{k=1}^{\infty} \frac{(-n)^k}{k!} \int_V d^3 y_1 \cdots d^3 y_k \xi_{k+2}(x_1, x_2, y_1, \dots, y_k), \end{aligned}$$

and the other  $\bar{\xi}(\cdot)$  are defined analogously (White, 1979; Balian & Schaeffer, 1989). Actually,  $\bar{\xi}(x)$  is independent of  $x$ , due to translation invariance, and  $n\bar{\xi}(x)$  can be interpreted as a density corrected by the presence of the neighbouring void.<sup>4</sup> This property can be used to rewrite Eq. (4) in a simpler fashion.

Following the procedure in Sect. 2.1.1, we can derive from Eq. (4) the expression for  $\mathbb{P}_0[V]$ . Unfortunately, it is a complex expression that depends in a complicated way on  $V$  and the angular coordinates, unlike in the Poisson case. However, in the Gaussian approximation ( $V \rightarrow \infty$ ), Eq. (4) simplifies and we can then specify the corrections to the Poisson formula

for  $\mathbb{P}_0[V]$ . Given that  $\xi_2$  is positive in the sphere, the correction to the density is negative. Thus, the sign of the total correction to the Poisson formula depends on the balance between this negative correction, the positive corrections provided by  $\xi_2(x_i, x_j)$ ,  $1 \leq i, j \leq 4$ ,  $i \neq j$ , and, in addition, the already considered correction to  $P_0[V]$  (which is positive). We notice that this result for the Gaussian  $\mathbb{P}_0[V]$  is different from and more complicated than the formula given by Betancort-Rijo (1990).

### 3.2. The cumulant expansion of the VPF and the nonlinear regime

We have seen that the Gaussian approximation fails when  $N = nV$  grows. In general, we may ask the radius of convergence of the power expansion in Eq. (2). It turns out that this expansion is not necessarily convergent, that is to say, its radius of convergence can be zero. For example, the expansion corresponding to the lognormal model is indeed not convergent but only asymptotic as  $N \rightarrow 0$ . In other words, it is only useful for computations as long as there is a sufficient number of decreasing terms. In particular, for given  $\bar{\xi}_2$ , the (asymptotic) convergence of that series is limited to  $N < \bar{\xi}_2^{-1}$ , namely, to the value of  $N$  that makes the magnitude of the second term of the series equal to the magnitude of the first term (for larger  $N$ , the terms increase in absolute value).

We can interpret the condition  $N < \bar{\xi}_2^{-1}$  as follows. Let us consider the number variance in the volume  $V$

$$\frac{\langle \delta N^2 \rangle}{N^2} = \frac{1}{N} + \bar{\xi}_2.$$

The condition  $N < \bar{\xi}_2^{-1}$  tell us that the Poisson fluctuations dominate over the correlations. If these are small, as in a Gaussian distribution, the Poisson fluctuations dominate, unless  $N$  is relatively large (when  $N = 10$ , the corrections are already important in the Gaussian example above, with  $\bar{\xi}_2 = 0.32^2 \approx 0.1$ ). In contrast, in a strongly correlated distribution  $\bar{\xi}_2 \gg 1$ , the Poisson fluctuations are only important in very small volumes.

We can illustrate the behaviour of the VPF cumulant expansion for the lognormal model in the nonlinear regime with an example. Let  $\sigma = 1 \Leftrightarrow \bar{\xi}_2 = e - 1 = 1.718$ ; then,

$$\begin{aligned} \ln P_0[V] = -N + 0.859141 N^2 - 2.32178 N^3 + 13.6475 N^4 - \\ 166.23 N^5 + 4350.12 N^6 - 257043. N^7 + 3.56058 \cdot 10^7 N^8 - \\ 1.18446 \cdot 10^{10} N^9 + 9.61505 \cdot 10^{12} N^{10} + O(N)^{11}. \quad (5) \end{aligned}$$

When  $N = 0.2$ , we have three decreasing terms, which yield  $P_0[V] = \exp(-0.184209) = 0.831762$ , to be compared with the value computed directly from Eq. (3),  $P_0[V] = 0.838853$ . Alternately, we can compare it with the Poisson value  $P_0[V] = \exp(-0.2) = 0.818731$ . If  $N = 0.01$ , then the series has more decreasing terms, namely, up to the seventh term. However, the sum of those terms yields  $-0.00991629$ , that is to say, essentially the same value as the first term, corresponding to a Poisson distribution. Thus, in the nonlinear regime, the sum of the decreasing terms of the series is a very small correction to the first term  $-N$  (the Poisson term). It is clear that the series expansion is then totally useless.

The non convergence of the cumulant expansion of the lognormal model is due to the slow decay of its density probability distribution function in the high density limit. In general, mass distributions that are singular on small scales possess probability distribution functions with fat tails in the high density limit. If the singularities are not too strong, the probability distribution

<sup>4</sup> This density is related to the cluster density by  $n\bar{\xi}(x) = n \frac{dn_c}{dn}$ .

function can have moments of any order, as the lognormal distribution does. Then, the series expansions of the moment generating function and of the void probability function are well defined, but they are asymptotic rather than convergent. Even when they exist, these cumulant expansions are not useful for practical purposes in the nonlinear regime.

### 3.3. Scaling in the nonlinear regime

In the strongly correlated regime  $\bar{\xi}_2 \gg 1$ , a systematic approach is provided by the assumption of scale invariance (or self-similarity). The fractal regime is characterized by strong scaling correlations. In particular, the mass fluctuations in a volume  $V$  in a fractal follow a power law, namely,  $\bar{\xi}_2 \sim V^{-\gamma/3} \gg 1$ , where  $\gamma$  is the scaling exponent of the two-point correlation function,  $\xi_2(r) \sim r^{-\gamma}$  (Gaité et al, 1999). Then, the correlation dimension of the fractal is  $3 - \gamma$ . On the other hand, it is natural to connect the VPF with the box-counting dimension: the former gives the probability of a region of size  $V$  (a box, say) being empty and the latter gives the asymptotic number of non-empty boxes of size  $V$  as  $V \rightarrow 0$ . The box-counting dimension is equal to the correlation dimension in a monofractal.

Let us take our sample to be defined in a region that we divide into a mesh of cells with volume  $V$  each. Then, the ratios of empty or non-empty cells give us estimations of  $P_0[V]$  or  $1 - P_0[V]$ , respectively. We may call the latter the non-void probability function. Its behaviour as  $V \rightarrow 0$  is related to the box-counting dimension of the distribution: the number of non-empty cells of size  $V$  is the power law  $V^{-D_b/3}$ , where  $D_b$  is the box-counting dimension and, therefore, the ratio of non-empty cells is also a power law, namely,  $V^{1-D_b/3}$ . This exponent is always non-negative and is zero only if  $D_b = 3$ . If the exponent is positive,  $P_0[V]$  tends to one. When  $D_b = 3$ ,  $P_0[V]$  is not constrained and the distribution can occupy any positive volume.

To analyse further the nonlinear behaviour of the VPF under the assumption of scaling, we need a particular model. Let us recall that the large deviation formulation of multifractals (Harte, 2001) allows us to connect them with the lognormal model, which can be regarded as a simple multifractal approximation (Gaité, 2007). We have the exact expression of the lognormal model VPF in Eq. (3). Now, let us also recall the scaling behaviour of density moments (Gaité, 2007):

$$\langle \rho^n \rangle = \langle \rho^n \rangle \sim V^{(n-1)D_n/3 + D_0/3 - n},$$

where  $D_n$  are Rényi dimensions and, in particular,  $D_0$  can be identified with  $D_b$ . The exact expression of the lognormal model moments is (Coles & Jones, 1991)

$$\langle \rho^n \rangle = \exp\left(n\mu + \frac{n^2\sigma^2}{2}\right).$$

Equating both expressions, we obtain

$$\mu + \frac{\sigma^2}{2} \approx (D_0/3 - 1) \ln V, \quad (6)$$

$$n\frac{\sigma^2}{2} \approx (D_n - D_0) \ln V/3, \quad (7)$$

valid in the limit  $V \rightarrow 0 \Leftrightarrow \mu, \sigma^2 \rightarrow \infty$ . If  $\mu = -\sigma^2/2 \Leftrightarrow \langle \rho \rangle = 1 \Rightarrow D_0 = 3$ , then a realization of the lognormal field occupies the maximum volume and  $P_0[V]$  vanishes. In general, the non-void probability function  $1 - P_0[V] \sim \langle \rho \rangle^{-1} \sim V^{1-D_0/3}$ , as explained above.

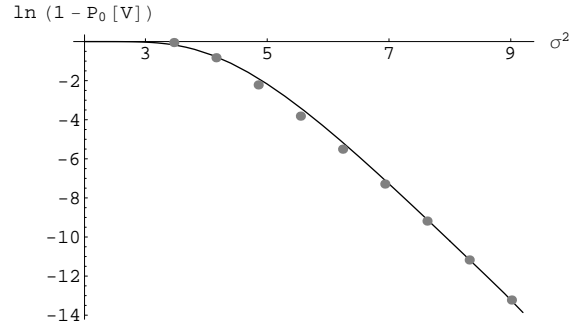


**Fig. 1.** Log-log plot of the nonlinear lognormal non-void probability function (note that  $\sigma^2 \propto -\ln V$ ). The parameters used in this plot correspond to the GIF2 cosmological simulation. The nine values are estimations from counts in cells in the GIF2 simulation.

Let us consider the scaling lognormal model with  $D_b = 3$ . In the strongly correlated regime, such that  $\sigma \gg 1$  while  $N$  stays finite,  $P_0[V]$  also approaches unity, according to Eq. (3). This limit is a consequence of the strong clustering of particles, which leaves too large voids, like when  $D_b < 3$ . The asymptotic behaviour  $\sigma \rightarrow \infty$  now yields

$$1 - P_0[V] = \frac{\sqrt{2N}}{\sigma} e^{-\sigma^2/8} + e^{-\sigma^2/8} \mathcal{O}(\sigma^{-2}). \quad (8)$$

Then, we deduce from Eqs. (7) and (8) that  $1 - P_0[V]$  is a power law (except for a small logarithmic correction), namely,

$$\log(1 - P_0[V]) \approx \left(\frac{1}{2} + \frac{\gamma}{24}\right) \log V, \quad (9)$$

where  $\gamma = 3 - D_2$ , again.

In Fig. 1, we have plotted  $\ln(1 - P_0[V])$ , as given by Eq. (3), versus  $\sigma^2 \propto -\ln V$ . We have used in the calculation for that plot parameters corresponding to the GIF2 cosmological simulation (Gaité, 2007):  $n = 400^3$ , and  $\sigma^2 = -(\gamma/3) \ln(nr_0^3)$ , where  $\gamma = 1$  and  $r_0 = 1/4$  is the scale of crossover to homogeneity in the distributions of halos. The scaling behaviour observed in the plot corresponds to  $\sigma^2 > 7$ . Unfortunately, this behaviour is not given by Eq. (9) but it is the Poisson behaviour, because  $N\bar{\xi}_2 < 0 \Leftrightarrow \sigma^2 > (3/\gamma - 1)^{-1} \ln(nr_0^3) \simeq 7$ . Indeed, the Poisson VPF for  $N \ll 1$  is such that  $\log(1 - P_0[V]) = \ln(nV)$ , which implies the constant slope observed in the plot. In Fig. 1 also appear nine values obtained by estimating  $P_0[V]$  from the count-in-cell analysis of the GIF2 simulation (Gaité, 2007). We can appreciate that the scaling lognormal model predicts correctly those values.

In the scaling lognormal model, all the Rényi dimensions  $D_n$  are functions of only two parameters, unlike in general multifractals, in which they are independent. However, Eqs. (6) and (7) encompass various types of fractal behaviour. For example, let us consider  $\mu \rightarrow \infty$  while  $\sigma$  stays finite. Then  $D_n = D_0$  for every  $n$ , which corresponds to monofractal behaviour. The non-void probability function  $1 - P_0[V] \sim \langle \rho \rangle^{-1} \sim V^{1-D_0/3}$  still vanishes, but the fluctuations of the distribution in the non-void cells are bounded (they can even be Gaussian). If  $\sigma \rightarrow \infty$  as well, the distribution in the non-void cells are unbounded, as in proper multifractals. In any event, the leading behaviour of the non-void probability function is given by  $D_0$ , unless  $D_0 = 3$ . We study the properties of general multifractal voids in Sect. 6.

#### 4. Detecting voids: a spherical void finder

The definition of voids in a point distribution is subtle and, to some extent, subjective (except in a one-dimensional distribution, of course). This question has been amply discussed and various void-finders have been devised, assuming different definitions of voids. These definitions include partially empty voids. For example, the popular void-finder devised by El-Ad & Piran (1997) begins with a “wall builder”, which separates “field galaxies” from “wall galaxies” to delimit voids. Then, it fits empty spheres, but the final voids are unions of spheres with different radii and have variable shape. Nowadays, several void-finders are available, mostly based on adaptable void shapes. We have introduced a void-finder based on discrete-geometry constructions that also defines voids of variable shape and we have demonstrated that this void-finder is capable of finding scaling in the void distribution (Gaité, 2005-B).

The separation of “field galaxies” that form a less clustered population is a useful previous step, but its application is connected with the notions of coexisting populations and galaxy biasing, which we study in detail in Sects. 6.5 and 7. It is also connected with a sophisticated type of voids, suggested by the scaling properties of multifractals and introduced by Gaité (2007). This type of voids is studied in Sects. 6 and 7.

In this section, we adopt the point of view of the preceding sections, based on simple void shapes. For example, constant-shape voids are such that only their size and orientation can change (apart from their position). In particular, if we use spheres, only their size can change. Let us mention that a widespread and more flexible alternative is the use of ellipsoids, whose shape can change but is defined by few parameters. In fact, ellipsoids are useful even as fits to more complicated shapes. However, their eccentricity (departure from the spherical shape) needs to be bounded above. Since the value of this bound is arbitrary, ellipsoids are less suitable than spheres for a universal definition of voids.

As we consider that discrete-geometry constructions are the right starting point, we first review the algorithm for variable-shape voids introduced in Gaité (2005-B) and then we introduce a new and simple algorithm for spherical voids, also based on discrete geometry constructions.

##### 4.1. Algorithm for variable-shape voids based on the Delaunay tessellation

Given a set of isolated points, a natural geometric construction associated with it is its Delaunay tessellation (Aurenhammer & Klein, 2000; van de Weygaert, 2002). This construction provides the *unique* set of largest empty balls associated with the set of points, such that each ball is defined as the circumscribed sphere to a Delaunay simplex (as a set of four non-coplanar points).

Thus, the algorithm devised by Gaité (2005-B) was meant to be natural and practical. It begins with the Delaunay simplices and joins adjacent simplices according to the overlap of their respective balls (Gaité, 2005-B). Therefore, this void-finder provides a set of polyhedral voids that tessellate the entire sample region; in other words, all the available space is assigned to voids. In particular, some of the found voids can be very small: the total range of sizes can span many orders of magnitude. This property is convenient for testing the scaling of voids. In fact, the void-finder demonstrates this scaling (Gaité, 2005-B).

However, this void-finder only works properly in fractals with dimension  $D$  larger than 2 (in three-dimensional ambient space). If  $D < 2$ , the voids tend to become degenerate, that is to

say, tend to depart from round shapes, and, when  $D$  is sensibly smaller than two, it is likely that one void percolates through the sample. This percolation of voids can be avoided by decreasing the overlap parameter, which controls the shape of voids (Gaité, 2005-B). Nevertheless, the value of the fractal dimension that the void-finder yields is always larger than two, because the boundaries of the voids have dimension two. This problem is better understood in terms of the notion of cut-out sets (Gaité, 2006), which we study in Sect. 5.1. Of course, other void-finders that define variable-shape and space-filling voids can also yield a fractal dimension larger than two.

In general, the only way to prevent the ambiguity due to the shape of voids is to prescribe voids of constant regular shape. We have shown that void-finders based on voids of constant shape demonstrate the scaling of voids in fractal distributions; namely, the rank-ordering of the found voids fulfills Zipf’s power-law (Gaité & Manrubia, 2002). Here, we propose an improved void-finder of this type.

##### 4.2. New algorithm for finding spherical voids

We have noticed that the scaling of voids is best realized when we impose that voids touch the fractal, that is to say, when we reject the voids that do not touch at least one point of the fractal (Gaité & Manrubia, 2002). Actually, we should demand that the set of constant-shape voids has maximal contact with the fractal. In the case of spherical voids, we can demand that each sphere is defined by four non-coplanar points on its boundary. This condition implies that each void is the sphere circumscribed to a simplex of the Delaunay tessellation of the sample. Therefore, this tessellation is also the primary element of a new and universal void-finder with no parameters. We further require that the balls are contained in the sample region and that they do not overlap. Thus, the algorithm begins by finding the largest ball in the sample region among those defined by the Delaunay tessellation, and proceeds by searching for the next largest non-overlapping ball, until the available balls are exhausted.

Although we are interested in the scaling of voids, this void-finder is applicable to any sample, in particular, to a sample of a uniform distribution. In this case, we can test the laws studied in Sect. 2. These laws refer to *all* the spherical voids in a sample, but the no-overlap condition restricts the set of voids. However, the sample of voids obtained under this condition is unbiased and, therefore, it has the same distribution as the total set of voids. To test it, we have generated a random set of 10000 points in the unit square and then run the void-finder. Its output (in rank order) is compared in Fig. 2 with the analytical prediction. This prediction results from the two-dimensional version of the distribution of voids  $\mathbb{P}_0[V]$  given by Eq. (1) (replacing volume  $V$  with area  $A$ ); namely, the rank is given by the cumulative probability  $\mathbb{P}_>[A] = (1 + nA) e^{-nA}$ . The agreement shown by Fig. 2 is remarkable.

We have also applied this void-finder to several samples of random Cantor-like fractals. We show in Fig. 3 the results corresponding to a random sample of 10000 points of a two-dimensional random Cantor-like fractal with  $D = 1.585$ . Note that the found circular voids (Fig. 3, top) do not cover the entire sample region (the unit square). In fact, they cover only 70% of it. Nonetheless, they convey well the notion of a hierarchy of voids.

In addition, we have tested this void-finder on random Cantor-like fractals that do not fulfill the condition  $D > d - 1$ , where  $d$  denotes the dimension of the ambient space ( $d = 2, 3$  in our tests). While finders of space-filling voids do not work or



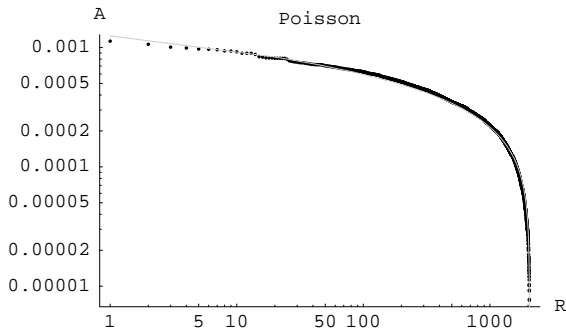


**Fig. 2.** Rank-ordering of the circular voids in a random set of 10000 points ( $A$  is the void area and  $R$  is the rank) compared with the predicted law (gray line).

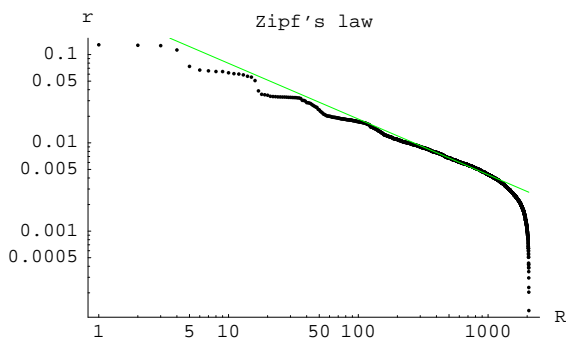
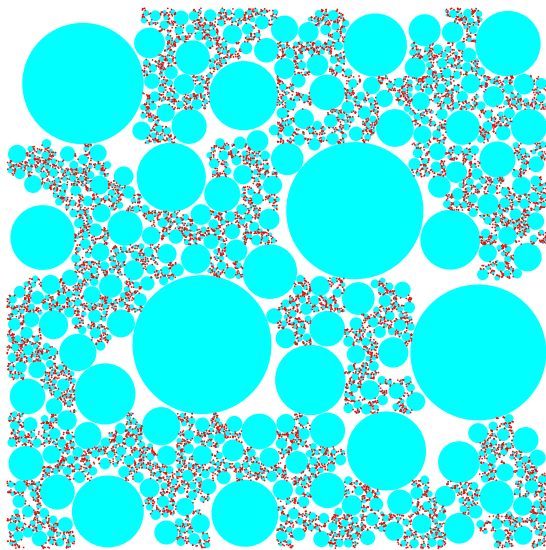


**Fig. 3.** (Top figure) Random Cantor-like fractal sample with 10000 points ( $D = 1.585$ ) and its corresponding voids found with the new algorithm (described in the text). (Bottom figure) Log-log plot of the rank-ordering of the void radii, compared with the straight line with slope  $1/D$ .

not find the right scaling when  $D < d - 1$ , our new void-finder works fine and obtains the approximate value of  $D$ . We explain the theory of non space-filling voids in the next section.

Finally, let us remark that the algorithm is very simple and indeed runs very fast.

## 5. Scaling of fractal voids

Scaling of voids is natural in a self-similar fractal: given that the fractal is the union of a number of smaller similar copies of itself,

every void also has smaller similar copies of itself, such that there is an infinite hierarchy of similar voids of decreasing size. The simplest example of this similarity of voids is the middle third Cantor set. It is desirable to generalize this argument to random self-similar fractals and to higher dimensions.

A self-similar distribution of voids fulfills the diameter-number relation  $N_{>}(\delta) \approx \delta^{-D}$ , namely, it is such that the cumulative number of voids with diameter larger than a given value is a power law, with minus the similarity dimension  $D$  as exponent (Mandelbrot, 1983). Given that  $N_{>}(\delta)$  is the rank  $R$  of the void with diameter  $\delta$ , the rank-ordering of void sizes is also a power law, that is, an instance of Zipf's law. A Zipf law is usually demonstrated as a constant slope in a log-log plot. The lengths of the gaps in the middle third Cantor set follow Zipf's law; in particular, its discrete scale invariance produces a staircase pattern in the log-log plot of the rank-ordering of those lengths. In random self-similar fractals, the cumulative probability of sizes of voids also follows a power law.<sup>5</sup> In three dimensions, scaling voids must fulfill the law  $\mathbb{P}_{>}[V] \approx V^{-D/3}$ .

The voids detected by various void-finders in random fractals indeed follow a power law rank order (Gaité & Manrubia, 2002; Gaité 2005-B). In practice, the Zipf law of voids constitutes a straightforward proof of fractality. However, the absence of a formal definition of voids in dimensions larger than one makes a rigorous study of the scaling of voids difficult. This was the motivation for introducing the notion of cut-out sets (Gaité, 2006).

Cut-out sets are obtained by removing from an initial region an infinite sequence of disjoint regions that exhausts the volume of the initial region (Falconer, 1997). These removed regions are the natural voids. The final structure is a sort of foam (under some conditions). Therefore, cut-out sets are relevant for “cosmic foam” models of large scale structure (Icke & van de Weygaert, 1987; van de Weygaert, 2002).

Fractals related to cut-out sets can be constructed with a modified procedure that permits void merging, in such a manner that the voids form just one connected region. For example, the fractal in Fig. 3 is of this kind. However, even more general fractals can have a meaningful sequence of voids, such as the sequence found with our spherical void-finder. In particular, that sequence can fulfill Zipf's law. This motivates us to extend our previous study of cut-out sets (Gaité, 2006) to more general fractals.

Connected with our generalization of cut-out sets is the notion of “fat fractal”. Sets with fractal structure but non-zero volume were studied by Mandelbrot (1983) and, later, they were called fat fractals (Grebogi et al, 1985). We can distinguish two types of fat fractals: (i) non-scaling fractals, namely, cut-out sets such that the sizes of their voids decrease faster than a power law, and (ii) cut-out sets with scaling voids that do not exhaust the initial volume. The latter type is relevant for sequences of non space-filling voids, which we study in Sect. 5.2.

In this section, we restrict ourselves to totally empty voids in continuous distributions. However, a finite fractal sample has, in addition, Poissonian fluctuations that can give rise to Poissonian voids, as studied in Sects. 2 and 3. We postpone the study of Poissonian voids to Sect. 6.

### 5.1. Cut-out sets and scaling of voids

Fractal cut-out sets are obtained by removing an infinite sequence of disjoint connected open regions from an initial com-

<sup>5</sup> Mandelbrot (1983) calls hyperbolic a power-law cumulative distribution. However, a more common name for it is Pareto distribution.



compact and convex region, in such a way that the sum of the removed regions tends to the volume of the initial region.<sup>6</sup> We can consider the voids in order of decreasing size and that every void is cut out from the remainder of the previous cuts. A well known one-dimensional example is the middle third Cantor set. In a sense, every closed fractal is a cut-out set, because its complement is open and, therefore, it is the union of a sequence of disjoint connected open regions.<sup>7</sup> However, there may only be a finite number of them. We regard as proper cut-out sets the closed sets with vanishing volume and an infinite sequence of cutouts (voids).

In one dimension, voids are necessarily open intervals. Thus, every closed one-dimensional fractal can be constructed like the Cantor set. In higher dimensions, a connected open region can have a very complicated shape; for example, it can have any number of “matter islands” and it can have a very rough boundary (a familiar image of a connected open region is provided by the shape of a cloud). Therefore, it is convenient to restrict ourselves to regular shapes and, in particular, to convex voids (Gaité, 2006). Under this condition and the condition that the voids do not degenerate to lower dimensional objects (along the sequence), the Zipf law of voids holds.

Let us mention a famous class of deterministic cut-out fractals with convex voids in two dimensions: the Sierpinski carpets. The triadic Sierpinski carpet is constructed as a sort of two-dimensional generalization of the middle third Cantor set: from an initial square, the middle (open) sub-square of side one third is cut out, and the iteration proceeds with the remaining eight sub-squares. It has  $D = 1.89$ . Variants of this construction produce other cut-out fractals with square voids (Mandelbrot, 1983). It is straightforward to generalize these constructions to three dimensions. All these fractals have discrete scale invariance and the log-log plots of the rank-orderings of their void sizes produce typical staircase patterns.

In contrast, fractals without discrete scale invariance can be generated by either deterministic or random algorithms, and are such that the size of their voids tends to decrease in a continuous fashion. For example, in the random fractal in Fig. 3, the (relatively smooth) steps on small ranks vanish on larger ranks. In general, we can express the scaling of voids as a particular power-law form of the rank order of diameters:  $\delta(R) \asymp R^{-1/D_b}$ , in terms of the relation  $\asymp$ , which means that the quotient between the related quantities is bounded above and below. This number-diameter relation is equivalent to a common form of Zipf’s law: the log-log plot of the rank ordering stays between two parallel lines with a slope given by the exponent  $(-1/D_b)$ , in the present case). Of course, if the sequence of voids is non-degenerate ( $V \asymp \delta^3$ ), we can replace  $\delta$  with  $V^{1/3}$  in the rank-ordering, and

$$V(R) \asymp R^{-3/D_b}. \quad (10)$$

<sup>6</sup> Let us recall some basic geometrical notions that are necessary here. Given a region in Euclidean space, its boundary is formed by points such that any ball centered on them intersects both the region and its complement. A closed set contains its boundary. If a closed set is bounded, it is also compact. An open set does not contain any boundary point. The complement of an open set is closed and vice versa. The union of open sets is open. A disconnected set can be divided into two parts such that each one is disjoint with the boundary of the other. A convex set contains every segment with ends in the set.

<sup>7</sup> This statement is a classic theorem of topology, proved by, e.g., Franz (1965).

A cut-out fractal is formed by the union of the boundaries of its voids.<sup>8</sup> Naturally, a cut-out set has fractal dimension larger than two (in three-dimensional space).<sup>9</sup> Cut-out sets with convex and non-degenerate voids formalise the geometry of fractal foams. For example, the voids can be convex polyhedra, like in the Voronoi foam model of Icke & van de Weygaert (1987). Besides, the mass may not be homogeneously distributed on the boundaries of voids. For example, the Voronoi foam model of Icke & van de Weygaert (1987) is based on the expansion of initial under-dense regions, which become depleted while the walls between them concentrate their mass. However, the evolution of the resulting foam continues with the motion of the matter in the walls towards their intersections to form filaments, and, then the motion along the filaments to form nodes.

To illustrate inhomogeneous cut-out sets, we can use a toy model inspired in the Sierpinski carpet, which we call the *Cantor-Sierpinski carpet*. We construct it with a slightly modified Sierpinski algorithm. The first step of the fractal generator consists in cutting out the middle sub-square of side one third from an initial square. We can describe this operation as a uniform displacement of mass from the middle sub-square to the surrounding sub-squares (as in a model of cosmic foam). Then, following the above-mentioned idea of a latter mass displacement along walls, we further concentrate part of the mass in the four sub-squares at the corners. Thus, the generator consists in the following way of dividing the total mass into the nine sub-squares: the central one receives nothing, the four sub-squares at the corners each receive a proportion  $p_1$  of the total, and the remaining four sub-squares each receive a proportion  $p_2 < p_1$ , with  $4(p_1 + p_2) = 1$ . The resulting inhomogeneous cut-out fractal is supported on the Sierpinski carpet but has maximal mass concentrations on the two-dimensional Cantor dust (the Cartesian product of two Cantor sets). The case  $p_1 = 1/6$ ,  $p_2 = 1/12$  is shown in Fig. 4. In fact, the Cantor-Sierpinski carpet is a multifractal, which we revisit in Sect. 6.

Now, let us consider a different modification in the construction of a cut-out set. It is easy to see that the boundaries of different voids can intersect one another. Then, it may be possible to remove a piece of common boundary so that the joined voids form a larger void, namely, a connected open region (which is not necessarily convex). With this merging prescription, the shapes of the voids become more complex and, in fact, all the voids may form a finite number of connected regions, or even only one region. Moreover, the modified (improper) cut-out set may not contain any piece of surface. A two-dimensional example of complete merging of voids is the fractal in Fig. 3. An ideal void-finder should be able to undo the merging, but there is no general procedure to recover a unique cut-out set structure and, hence, a unique set of voids.

On the other hand, if the dimension of a (closed) fractal is smaller than two, then it cannot be constructed as a (proper) cut-out set: its complement (in the region where the fractal is defined) is connected.<sup>10</sup> Then, in the absence of a natural void structure, it does not make sense to try to find “real” fractal voids

<sup>8</sup> To be mathematically rigorous, a cut-out set is the boundary of the union of its voids rather than the union of the boundaries of its voids. The former is usually larger than the latter and is actually its closure, namely, the smallest closed set that contains it. This subtle difference is irrelevant regarding its box-counting dimension but is relevant regarding its Hausdorff-Besicovitch dimension.

<sup>9</sup> A rigorous proof of this fact involves the notion of topological dimension (Mandelbrot, 1983).

<sup>10</sup> We assume that the region where the fractal is defined is a given simple region, preferably convex. By default, we assume a cube. If no

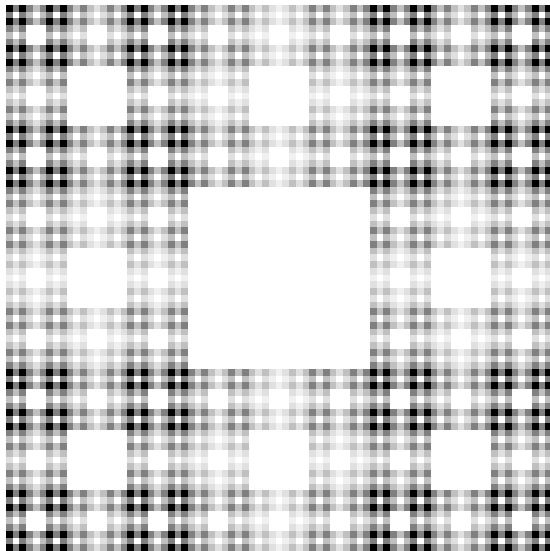


**Fig. 4.** Two-dimensional inhomogeneous fractal foam: the Cantor-Sierpinski carpet. It is a multifractal cut-out set: beside the empty voids corresponding to the Sierpinski carpet, we can perceive very low density regions, in contrast with the mass concentrations near the two-dimensional Cantor dust.

by using a space-filling void-finder, and it may be more sensible to look for equal-shaped voids, as we have argued in Sect. 4. Therefore, we are going to explore how to generalize the relation between the scaling of voids and the fractal dimension to voids that touch a fractal but do not totally fill its complementary region (like the circular voids in a square shown in Fig. 3).

## 5.2. Scaling and dimension provided by non space-filling voids

Let us consider a sequence of voids that touch a fractal but do not totally fill the fractal's complement. If every point of the fractal touches a void, the fractal is included in the boundary of the voids. Mandelbrot (1983) studied self-similar unions of boundaries, especially, in two dimensions, under the name of sigma-loops (sigma-loop = sum of loops). As self-similar objects, they are constructed by means of a generator, constituted by a number of parts; each part is substituted by a copy of the whole (scaled down by some factor). To such construction one can associate the similarity dimension  $D_s$ , namely, the quotient of the logarithm of the number of parts by the logarithm of the inverse of the similarity ratio. Mandelbrot (1983) measures every loop by its linear scale  $\delta$  (its diameter) and shows that the number of loops fulfills the diameter-number relation  $N_{>}(\delta) \asymp \delta^{-D_s}$ . The generalization to three dimensions (in terms of sigma-surfaces) is straightforward.

If a fractal is not exactly self-similar or if it does not coincide exactly with the boundary of its voids, Mandelbrot's treatment is not applicable. However, the method of Falconer (1997), extended by Gaité (2006), can be applied with some modifications. Let us recall that the method of Falconer (1997) is based on the equality of the box-counting dimension  $D_b$  and the Minkowski-Bouligand dimension. The latter dimension expresses the power-law behaviour, as  $r \rightarrow 0$ , of the volume  $V(r)$  of the  $r$ -neighbourhood of the fractal, which is the union of the

natural region is available, we can take the *convex hull* of the fractal, namely, the smallest convex set that contains it.

balls of radius  $r$  with centers in the fractal. The rank-ordering of voids provides bounds to  $V(r)$ , hence allowing one to connect the decrease rate of the volumes of voids with the decrease rate of  $V(r)$ .

Following the proof for cut-out sets, we can try to carry out the proof for general convex voids, instead of only equal-shaped voids (or balls). Let us assume the rank order of the diameters of the voids to be  $\delta(R) \asymp R^{-a}$ , with exponent  $a$ . We look for bounds to  $V(r)$  in terms of the voids. The lower bound to  $V(r)$  is independent of whether or not the voids are space-filling: the  $r$ -neighbourhood of the fractal is certain to contain every void with diameter smaller than  $r$ , because the voids touch the fractal. Then, the total volume of the voids fully included in that  $r$ -neighbourhood provides a lower bound to  $V(r)$  that implies  $D_b \geq 1/a$ .

To obtain an upper bound to  $D_b$ , we need an upper bound to the volume  $V(r)$ . However, the method of Gaité (2006) for cut-out sets needs modifications, because a good part of the  $r$ -neighbourhood of the fractal is now not included in the voids but in its complement (a fat fractal). Instead, we can appeal to the more general (but more complex) results of Tricot (1986, 1989). Tricot proves that the open sets packing the complement of the fractal can be quite general. This generality implies that the scaling of voids is not necessarily connected with the box-counting dimension  $D_b$ , like in cut-out sets, but it can be connected with a different type of dimension, the so-called *exterior capacity* dimension, which can be more appropriately called here the *interior* dimension of the voids.

Finally, let us notice that our algorithm does not guarantee that every point of the fractal belongs to the boundary of a void: each initial ball is defined by four points on its boundary, but many balls are removed to satisfy the non-overlap condition. The points of the fractal not included in the boundary of the voids, namely, the points that do not touch voids, can also make a contribution to the fractal dimension, if their relative weight is non-negligible, increasing the difference  $D_b - 1/a \geq 0$ . Nonetheless, the equality  $D_b = 1/a$  seems to hold for random self-similar fractals. Indeed, our tests on simulations show that the algorithm yields the right dimension, even when the fractal dimension is smaller than two.

## 6. Voids in a multifractal

Mandelbrot (1983) was concerned with the size and aspect of fractal voids in the distribution of galaxies. In fact, he favoured small voids in this distribution. Thus, he introduced the concept of fractal lacunarity and proposed that the galaxy distribution is a fractal with low lacunarity. Mandelbrot (1983) actually showed that fractals with the same dimension can look very different, according to their lacunarity. Finally, he presented a brief study of the Besicovitch fractal, which has been later described as a self-similar binomial multifractal. Mandelbrot (1983) called it instead a “non-lacunary” fractal, alluding to the fact that it has no open voids. The modern literature about multifractals is not particularly concerned with their voids, but the structure of multifractal voids indeed has interest in cosmology.

In a multifractal, the mass surrounding a point  $x$  grows as a power law with an exponent that varies with the point,  $\alpha(x)$ ; namely,  $m[B(x, r)] \asymp r^{\alpha(x)}$ , where  $m[B(x, r)]$  is the mass in the ball of radius  $r$  centered on  $x$ . This definition makes sense for points such that  $m[B(x, r)]$  is nonzero for all  $r > 0$ . These points form the support of the distribution, which is necessarily a closed

set.<sup>11</sup> A multifractal possesses a spectrum of dimensions, such as the set of local dimensions  $\alpha(x)$  or the set of Rényi dimensions  $D(q)$ ,  $-\infty < q < \infty$  (Harte, 2001). The box-counting dimension  $D_b$  of the multifractal support can be identified with  $D(0)$ .

A *monofractal* is defined as the particular case in which the local dimension  $\alpha$  is constant throughout its support. In other words, a monofractal is a uniform mass distribution with fractal support.<sup>12</sup> Of course, the dimension of the support coincides with the local dimension  $\alpha$ .

The notion of a void must be more complicated in multifractals than in monofractals, because of the spectrum of dimensions. To study in detail the nature of voids in multifractal distributions, we need to reconsider the definition of fractal voids. We can actually distinguish two types of voids.

### 6.1. The two types of voids in a multifractal

In Sect. 5, we have defined a void as a connected open region (which it is useful to consider convex). However, a multifractal can have a different type of voids. To introduce it, let us consider the example of the one-dimensional adhesion model. In this model, the mass concentrates in *shocks* and their locations form a countable but *dense* set (She, Aurell & Frisch, 1992; Vergassola et al, 1994); namely, in any interval, however small, there are shock points. Since the set of shock points is countable, it has null length, so the total length of the interval actually belongs to its complementary set. Therefore, this complementary set contains no mass and has non-vanishing length, but it does not contain any open void, because the shock points are dense.

Thus, it is too restrictive to require that voids be open. Indeed, in the adhesion model, every finite sample of the mass distribution displays voids (She, Aurell & Frisch, 1992; Vergassola et al, 1994). The mass distribution in the adhesion model is actually of multifractal type. A general self-similar multifractal mass distribution also has an infinite number of mass concentrations, with local dimension  $\alpha(x) < 3$  and diverging density. Moreover, these singular mass concentrations are dense in the support of the mass distribution; namely, any open region (or any ball) contains mass concentrations. Among the regular points, with a well-defined density, the points that we naturally assign to voids are the ones with local dimension  $\alpha(x) > 3$  and vanishing density (Gaité, 2007). Thus, the set of points with vanishing density has non-vanishing volume (indeed, it usually holds the total volume), but it may not contain any open set.

Therefore, we are going to distinguish two types of voids in general continuous mass distributions. The first type of voids consists in open regions. There can be one, many or an infinite sequence of void open connected regions. Their complementary region is closed and constitutes the distribution support. If there are no voids of that type, in other words, if the distribution support occupies the total volume in which the distribution is defined, we must consider a more general type of voids: the set of points with vanishing density. Of course, the density is also zero in open voids, but we demand that voids of the second type belong to the support of the mass distribution. Both types of voids

are present in some self-similar multifractals, for example, in the Cantor-Sierpinski carpet (Fig. 4).

In general, multifractal distributions may or may not have voids of the first type but they certainly have voids of the second type, which are the proper multifractal voids. However, the large density fluctuations inherent to multifractals imply that the distinction between both types of voids gets blurred in finite samples, in which the voids are Poissonian. This remark is important, of course, for the application to real data. Then, the only way to determine the type of voids is by increasing the sample density  $n$ , so that voids of the second type get filled.

When we consider finite samples, a coarse-grained version of the mass distribution is adequate to study the geometry of voids. Let us see that the distinction between the two types of voids disappears in coarse-grained mass distributions.

### 6.2. Connection with excursion sets

Self-similar multifractal mass distributions have a dense set of singular mass concentrations where the density diverges. To remove these singularities, it is convenient to coarse-grain the distribution, for example, using a window function or low-pass filter of wave-numbers. Then the mass density is well defined everywhere. The lognormal model, already employed in Sect. 3, is a suitable coarse-grained approximation to self-similar multifractal mass distributions (Gaité, 2007). A density field allows us to define voids as the regions where the density is below some given threshold. This definition has been introduced by Sheth & van de Weygaert (2004) and by Shandarin, Sheth & Sahni (2004).

On the other hand, a coarse-grained continuous distribution can be obtained from a finite sample and, if the coarse-graining length is well chosen, it is a good description of it. Regarding voids, the appropriate coarse-graining length is such that, in average, there is one particle in a volume of that length ( $N = 1$ ). Thus, under-dense regions are real voids (Gaité, 2007).

A density field resulting from coarse-graining is continuous (in general). This implies that excursion sets are open sets, if they are defined as the points where the density is strictly smaller than a given value (say the average density). Therefore, their geometry is similar to the geometry of multifractal voids of the first type. As we have already mentioned, every open set is formed by a sequence of connected open regions. Every connected open region constitutes an individual void. This geometry is simpler than the geometry of multifractal voids of the second type. However, let us emphasise that a connected open region can be very complex.

For illustration, we have computed excursion sets of a realization in a square of a two-dimensional lognormal field with  $\langle \rho \rangle = 1$  and  $\sigma = 1.65$ . We have plotted in Fig. 5 the excursion set corresponding to the average density (one). The black region is the excursion set, which can be decomposed into a set of connected regions that constitute individual voids. A good part of the total volume belongs to the largest void, which percolates through the square. There are smaller voids as islets inside the matter clusters (“voids in clouds”). Unlike in a Gaussian field, there is no symmetry between clusters and voids. The matter clusters contain most of the mass but have small total volume. Indeed, the matter clusters occupy only 20% of the volume but hold 80% of the total mass. Since the matter clusters occupy a small but non-vanishing volume, we can regard them as a fat fractal.

The largest connected void in Fig. 5 illustrates the complicated geometry that a connected open region can have (a geom-

<sup>11</sup> Indeed, the support of a mass distribution is precisely defined as the smallest closed set that contains all the mass.

<sup>12</sup> To be precise, the uniformity *only* affects the exponent. The prefactor in the power law can vary, giving rise to different monofractal distributions with the same support and exponent, but with different (bounded) inhomogeneities in the support.

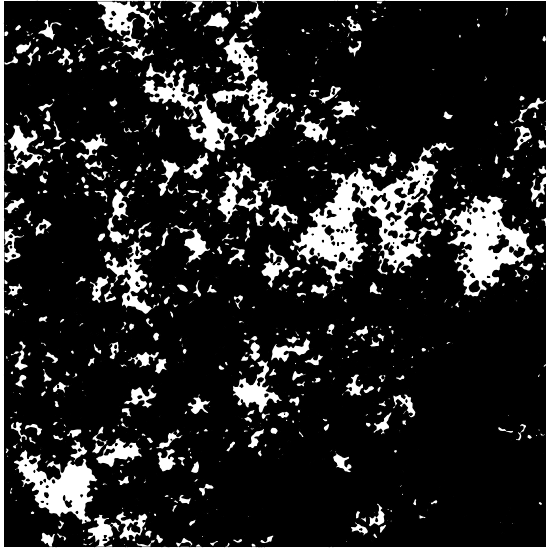


**Fig. 5.** Voids (in black) defined by the average-density excursion set of a lognormal model.

etry that can be even more complicated in three dimensions). It seems natural to divide a void like that into smaller but simpler regions. A natural way to do it is by choosing the smaller regions convex, like we did in cut-out sets. Then, we understand that the total connected region is constructed by merging the smaller convex regions. However, a careful look at Fig. 5 will convince us that the necessary number of convex components of the largest void is huge.

From Fig. 5, we can imagine the geometry of voids of the second type. When the coarse-graining length decreases, more and more matter halos pop up in the voids and more and more voids pop up in the matter clusters, as the mass distribution becomes more singular. In an  $N$ -body cosmological simulation, Gottlöber et al. (2003) re-simulated voids with higher resolution and indeed observed the formation of small halos in them in a self-similar pattern. In the limit of vanishing coarse-graining length, halos (mass concentrations) are fully mixed with (are dense in) some parts of the voids, which form voids of the second type. The open voids that may remain constitute voids of the first type. Moreover, voids occupy an increasing fraction of the total volume that tends to one, and contain a decreasing fraction of the total mass that tends to zero.

### 6.3. Scaling of voids in a multifractal

We have shown in Sect. 5 that fractal voids of the first type follow a diameter-number relation (under some conditions) and its exponent is given by the box-counting dimension  $D_b$  of the fractal. A multifractal possesses a spectrum of dimensions; in particular,  $D_b$  can be identified with the Rényi dimension  $D(0)$ . In Sect. 3.3, we have related  $D_b$  to the VPF. If  $D_b = D(0) < 3$ , then the support of the distribution is fractal, and the volumes of the corresponding first type voids scale according to Eq. (10). However, when  $D(0) = 3$ , the voids cannot satisfy Eq. (10): it would tell us that the total volume of the voids  $\sum_R V(R)$  diverges.

Actually, the case  $D(0) = 3$  is particularly important in our context, because the mass distributions obtained in  $N$ -body simulations of CDM models are consistent with  $D(0) = 3$  (Gaité, 2007). Furthermore, the supports of those distributions seem to be their entire regions of definition, such that there are no voids

of the first type. However, this conclusion is far from being certain. To confirm it, it is necessary to analyse simulations with larger ratios of the homogeneity scale to the discretization scale.

Regarding voids of the second type (non open), they have a very complicated geometry, as we have explained above. Indeed, the geometry of such voids is hard to describe. There can be an uncountable number of connected components or only one. In any event, it is very difficult to establish the sizes of separate voids and they may not be rank ordered. In particular, if there is an uncountable number of connected voids, it is possible that every separate void has zero volume, in spite that their total volume is positive. This happens in the one-dimensional adhesion model.

However, the radical differences between second type voids and open voids disappear when we consider a finite fractal sample. A finite sample naturally concentrates in regions with local dimension  $\alpha(x) < 3$  (halos), whereas voids are depleted (Gaité, 2007). Therefore, one can perceive more or less regular void shapes in a multifractal sample, even in the absence of voids of the first type. In fact, a finite multifractal sample can be described in terms of a coarse-grained mass distribution and its voids can be described in terms of excursion sets. However, we have seen that excursion sets are still complex. Therefore, it is convenient to define a sequence of convex voids by means of a void-finder; in particular, we can use the sequence of spherical voids found with the algorithm in Sect. 4. We have studied in Sect. 3.3 scaling features related to the VPF. We study the scaling of multifractal voids below.

### 6.4. Poissonian voids in a multifractal

For simplicity, we consider here only multifractals supported in their entire domains of definition, that is to say, such that they only have voids of the second type. A discrete sampling of a continuous distribution gives rise to Poissonian voids, as we studied in Sect. 3. Since the perturbative methods in that section are not applicable to multifractals, we study here the distribution of the voids in simulated random self-similar multifractals. In particular, we study a random self-similar multifractal with  $D(0) = 3$  and no open voids, employing the void-finder described in Sect. 4.2.

We analyse two-dimensional random multinomial multifractals (Harte, 2001). We define a particular multifractal in the unit square, with great precision; namely, we define about  $2.8 \cdot 10^{14}$  “pixels” (allowing us to specify coordinates with seven decimal digits). This multifractal has support in the whole unit square and, therefore, it has no voids of the first type. We have generated a sample of this multifractal with 10000 points (the typical order of magnitude of galaxy VLS’s). The application of our void-finder to this sample yields some (Poisson) voids with relatively large size (see Fig. 6). For example, the largest void has a radius equal to 0.0484 and an area equal to 0.00736 (in box-size units). According to the results of Sect. 2, the expected number of voids of that size in a sample of the uniform distribution with 10000 points, such that  $N = 73.6$ , would be  $10000 \cdot 73.6^2 \exp(-73.6) \approx 6 \cdot 10^{-25}$ . Naturally, this small number shows how inhomogeneous this multifractal is. Regarding the distribution of voids, the log-log plot rank-ordering of the sequence of void radii does not fulfill Zipf’s law (see Fig. 6).

We have also tested samples with different numbers of points. Smaller samples, namely, with less than 10000 points, have larger voids, but the total number of voids decreases. Of course, the rank-orderings of these reduced sequences of voids do also not follow a Zipf law. Larger samples have more voids,

with smaller size (which can be very small). Therefore, larger samples are more influenced by the error due to the finite precision of the multifractal measure. We have not observed any scaling range. In fact, the aspect of the log-log plots for all these rank-orderings (e.g., Fig. 6, bottom plot) is not unlike the aspect of the plot that corresponds to the Poisson field (Fig. 2).

Regarding the high number density of dark matter particles, totally empty spherical voids in their distribution must be very small. Therefore, it is more practical to consider spherical voids in the distributions of mass concentrations (halos), rather than in the raw mass distribution, following the ideas proposed by Gaité (2005-A, 2007). Voids in the distribution of halos can be related to voids in the distribution of galaxies, as we explain later.

### 6.5. Voids in a sample of uniform halos

According to the conclusions of Gaité (2007), some scaling properties of a self-similar multifractal may not be realized even in large samples. For example, the scaling of the two-point correlation function is not realized in  $N$ -body CDM simulations of current size (many millions of particles). Consequently, it is necessary to carefully select the most adequate scaling quantities. In particular, a well-motivated selection consists in the choice of quantities corresponding to a uniform halo population, namely, corresponding to a given local dimension  $\alpha < 3$ . If halos are realized by coarse-grained lumps of a given size, a uniform halo population consists of halos with similar mass. We expect that the voids in each population have better scaling properties, like do the correlation functions of each population (Gaité, 2005-A, 2007). We use the preceding multifractal to test this hypothesis.

To do the test, we need a sample with many more than 10000 points to coarse-grain them into a sensible number of halos. Therefore, we have generated a sample with 67 108 864 points. We have coarse-grained it in a  $1024 \times 1024$  mesh. We have selected the halos with a number of particles between 450 and 550, corresponding to  $\alpha \approx 1.7$ ; the resulting number of halos is 7548.<sup>13</sup> Then we have proceeded with these halos like with ordinary particles, namely, we have applied our void-finder and studied the void distribution. The results are shown in Fig. 7.

The voids in this set of halos are larger than the voids in the raw particle distribution (see Fig. 6). The reason for it is double: the set of halos is more clustered than the raw particle distribution, and, also, there are fewer halos now (7548) than particles in the above sample (10000). Now, the largest void has a radius equal to 0.0763. Regarding all the voids, the largest voids are now larger but they are located in about the same places. The sequence of voids now spans a larger size range, and its distribution is a little different from that of the voids of the basic particle population: a tentative fitting of a Zipf law yields a better result (Fig. 7). However, it is questionable that our selection of a uniform halo population approaches scaling behaviour. This result is to be contrasted with the clear scaling of correlation functions that is achieved by the selection of uniform halo populations (Gaité, 2005-A, 2007).

Let us notice the relation of the above selection procedure to the “wall builder” phase in the void-finder of El-Ad & Piran (1997). Indeed, their procedure also separates (galaxy) populations according to their clustering, although in a less discriminatory way: it only separates lowly-clustered “field galaxies”

<sup>13</sup> The value  $\alpha \approx 1.7$  is slightly smaller than  $\alpha_1 \approx 1.73$ , the local dimension of the mass concentrate of this distribution. This local dimension is, in general, such that  $\alpha_1 = f(\alpha_1)$ , that is to say, such that it coincides with the Hausdorff-Besicovitch dimension of the concentrate.

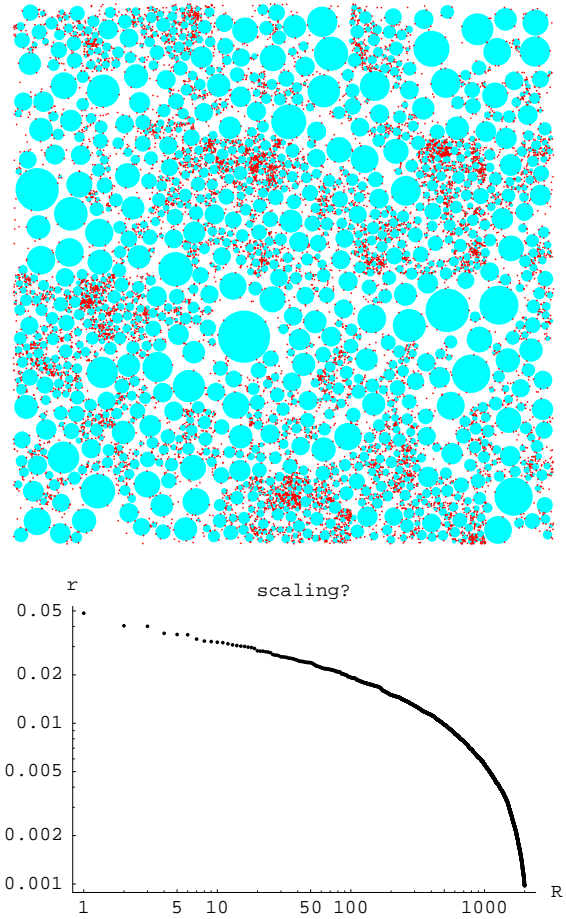


**Fig. 6.** Random multifractal sample with 10,000 points and its corresponding voids (top figure) found with the new algorithm. Log-log plot of the rank-ordering of the void radii (bottom plot).

from highly-clustered “wall galaxies.” Actually, their criterion for the separation of galaxies should coincide with a sort of discrete adaptation of a simplified version of our criterion for halos: to separate two populations according to their values of  $\alpha$ , we must just prescribe a threshold, such that the values below it are lowly-clustered while the values above it are highly-clustered. Since the local dimension  $\alpha(x)$  measures the concentration of mass around  $x$ , the mass in the ball of radius  $r$  centered on  $x$  is  $m[B(x, r)] \sim r^{\alpha(x)}$ . A discrete version of  $m[B(x, r)]$  is given by the number of points inside  $B(x, r)$ . A threshold for  $\alpha$  sets a threshold for this number, as El-Ad & Piran do.

## 7. Voids in galaxy samples and galaxy bias

Let us recall the observational evidence of scaling of sizes of galaxy voids, in particular, the study of voids in the 2dF survey by Tikhonov (2006) mentioned in Sect. 2.2.1 regarding the significance of large voids. Tikhonov performs the rank-ordering of voids in the mentioned VLS and indeed concludes that there is a scaling range. This range is about a decade, namely, an order of magnitude in the rank (from rank 60 to rank 600, approximately). Tikhonov (2006) uses his own void-finder, which first fits the largest empty spheres and then applies a merging criterion that allows the voids to become non-spherical (in a similar way to El-Ad & Piran, 1997).

The void-finder defined in Sect. 4 is simpler, for it only finds empty spheres, without merging them. We have applied



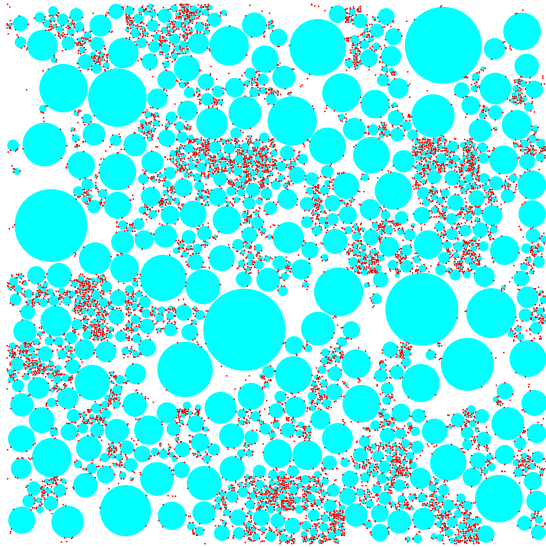


**Fig. 7.** Set of 7548 multifractal halos with masses between 450 and 550 particles, and its corresponding voids (top figure). Log-log plot of the rank-ordering of the void radii (bottom plot), in comparison with the straight line required by the Zipf law (corresponding to the dimension  $D = 1.7$ ).

our void-finder to Tikhonov’s VL sample.<sup>14</sup> The resulting rank order is plotted in Fig. 8. The range of radii is similar to the range found by Tikhonov, although somewhat larger at the lower end (which is not significant). However, no scaling range can be discerned in that plot.

We must also consider that previous analysis of galaxy catalogues have not revealed scaling of sizes of voids (Gaité & Manrubia, 2002). Indeed, it has not been clear if we should really expect this scaling. Our argument for scaling (Gaité & Manrubia, 2002) actually assumed a monofractal distribution of galaxies. Therefore, the voids in it should be of the first type, in our present classification. However, regarding that the distribution of galaxies is better described as a multifractal, the scaling of voids can be more complex, as we have discussed above. To draw conclusions for galaxy voids from our study of multifractal voids, we need to consider in detail the relation between the dark matter and galaxy distributions.

<sup>14</sup> Actually, we have removed a few galaxies from one boundary to make it straight, thus making the geometrical shape of the sample rectangular (in the angular coordinates). Furthermore, we have shifted slightly the position of the straightened edge in order to have a round number of galaxies in the sample, namely, 7000 (out of the initial 7219).

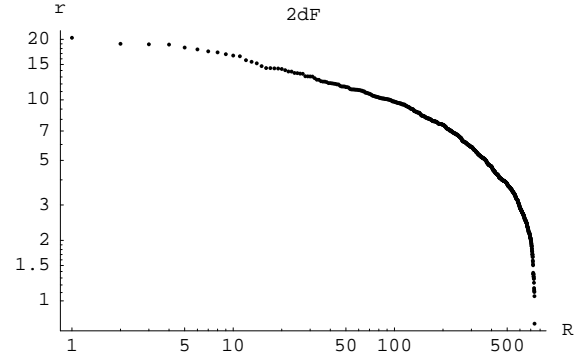


**Fig. 8.** Rank-ordering of the voids in Tikhonov’s 2dFGRS sample with 7000 galaxies ( $r$  is the void radius in Mpc.  $h^{-1}$ ).

### 7.1. Multifractal model of galaxy bias

One might assume that galaxies just trace the dark matter distribution, namely, that they constitute a fair sample of this distribution, considered continuous (“galaxies trace mass”). Any more sophisticated prescription amounts to galaxy biasing. Galaxy biasing is natural, since the principles that rule the distribution of galaxies are complex (indeed, the formation of galaxies is not well understood yet). There are various models of galaxy biasing. Our model combines the ideas of the “peak theory” of Gaussian fields (Kaiser, 1984; Bardeen et al, 1986) with our multifractal halo model (Gaité, 2005-A, 2007).

In a Gaussian field, the density is well defined everywhere. In contrast, in a singular distribution, in particular, in a multifractal, the density is not defined (it is, actually, infinite) in a large set of points. These points are mass concentrations, characterized by their local dimensions  $\alpha(x)$ . Therefore, we must substitute the density threshold employed to define peaks of Gaussian fields by a local-dimension threshold. This substitution becomes an actual equivalence if we coarse grain the singular distribution: then, the coarse-grained density measures the local-dimension. However, the coarse-grained density field is not Gaussian while the coarse-graining length is small (in the nonlinear regime).

Of course, the natural threshold is  $\alpha(x) < 3$ , which is just the definition of halos as mass concentrations proposed by Gaité (2005-A, 2007). The local dimension  $\alpha = 3$  corresponds to a coarse-grained density similar to the average density (in the support of the distribution). Therefore, the simplest model of galaxy biasing consists in that every halo hosts a galaxy with mass (or luminosity) proportional to the mass of the halo. Thus, the distribution of galaxies of given luminosity has a well defined fractal dimension. An important consequence of this model is that the total distribution of galaxies is also multifractal. This consequence can be tested in galaxy correlation functions. In fact, Zehavi et al (2005) and Tikhonov (2006) have found that the slope  $\gamma$  of the log-log plot of the two-point correlation decreases with luminosity in a way that agrees with a multifractal distribution of galaxies.

The value of the threshold is relevant for the definition of “wall galaxies”, as we comment in Sect. 6.5 regarding halos. Assuming that every halo hosts a galaxy, we can set a lower  $\alpha$  threshold (higher density threshold) for “wall galaxies”. A natural choice is the local dimension  $\alpha_1$  of the mass concentrate, such that  $\alpha_1 = f(\alpha_1)$ , which is the fractal (Hausdorff-Besicovitch) dimension of the concentrate. This choice ensures that the mass of all the “field galaxies”, corresponding to  $\alpha_1 < \alpha < 3$ , is almost negligible.

In any event, if every halo hosts a galaxy with luminosity proportional to the mass of the halo, the voids in a population of galaxies of given luminosity coincide with the voids in the parent halo population. Therefore, we can extend the conclusions of the study of voids in samples of uniform halos performed in Sect. 6.5 to galaxy voids; namely, the voids (of the second type) in them span a large range of sizes and their rank-ordering is vaguely similar to a Zipf's law.

For the sake of completeness, let us mention a more elaborate model of galaxies in dark matter halos that assumes that a halo can host more than one galaxy (see, e.g., Peacock and Smith, 2000). However, if the distribution of galaxies in a given halo follows the distribution of the dark matter in it, this model should be equivalent to the simpler model with only one galaxy per halo, provided that the dark matter distribution is multifractal. The reason for this equivalence is that the size of halos in the multifractal halo model is given by the chosen coarse-graining length, which can run within some limits without altering anything, due to the scale invariance (Gaité, 2007). Therefore, an increase in the size of halos must indeed correspond to placing more galaxies per halo, without altering their distribution.

Of course, the present observational limitations do not allow us to fully test these models or to determine the nature of galaxy voids. For example, we cannot tell how much matter the present voids contain or exactly in what form. In particular, small dark matter halos in voids are undetectable. Galaxy VLS's are naturally biased towards the more luminous populations. Thus, their voids do contain galaxies. In general, the observed voids seem to contain dwarf or low surface brightness galaxies. Peebles (2001) discusses the nature of void objects.

Finally, let us note that the various rank-orderings of voids in galaxy VLS's available agree qualitatively with a multifractal model of galaxy bias; namely, the corresponding log-log plots look like those in Fig. 6 or Fig. 7. Nevertheless, it is remarkable that some analyses seem to really demonstrate scaling, unlike our plots. This could hint at a more complicated model of galaxy biasing or at a dark matter distribution with totally empty scaling voids.

## 8. Discussion and Conclusions

The traditional Poissonian analysis of voids, based on the perturbative void probability function, is only valid when the Poisson fluctuations dominate over the correlations ( $N\bar{\xi}_2 < 1$ ). Thus, if there is more than one object per volume of the size of the homogeneity scale ( $N > 1$  when  $\bar{\xi}_2 = 1$ ), then the Poissonian analysis is only valid in the nonlinear regime. In particular, the Gaussian approximation can only be used, if at all, for very sparsely distributed objects, like Abell clusters or very luminous galaxies.

In the nonlinear regime, when the perturbative Poissonian analysis is valid, it yields no information. To obtain information in the nonlinear regime, we assume scale invariance of the correlation functions. Then, essentially two different situations are possible, according to the behaviour of the void probability function in the continuous distribution, namely, in the limit of infinite sampling density ( $n \rightarrow \infty$ ). When the box-counting dimension of the distribution is smaller than three, the void probability function approaches unity as the cell volume  $V \rightarrow 0$ . This happens, for example, in a monofractal. Conversely, if the void probability function of the continuous distribution does not approach unity as  $V \rightarrow 0$ , then the box-counting dimension of the distribution is three. Moreover, if the void probability function vanishes, a random cell is surely non-empty and normal voids are absent in the continuous distribution. In other words, voids are present

only while the sampling density  $n$  is finite (Poissonian voids). This Poissonian void probability function approaches unity as  $V \rightarrow 0$  and is related to a different Rényi dimension. The various behaviours of the void probability function are well illustrated by the scaling lognormal model.

Relying on previous work and for the sake of analytical simplicity, we have used empty spherical voids. Thus, we can carry out a complete analysis of voids in the Poisson distribution and a partial analysis in correlated distributions. We have designed a new and simple finder of non-overlapping spherical voids. We have tested it on Poisson distributions and ordinary fractal distributions, obtaining the expected rank-orderings of voids, namely, the analytical Poisson law and the Zipf law, for a random point distribution and a random Cantor fractal, respectively. The random fractal illustrates the aspect of spherical voids in a continuous mass distribution: they do not fill the void space but constitute a good approximation to a partition of it.

Focusing on continuous distributions, the scaling of voids is best studied by introducing the notion of cut-out sets. This notion is very general and every monofractal is, in a sense, a cut-out set. Mandelbrot's diameter-number relation can be translated into a power-law rank-ordering of void sizes (Zipf's law). Cut-out sets with non-degenerate convex voids formalise the geometry of fractal foams. Non-convex voids can be formed from convex voids by a process of merging. However, given a non-convex void, it cannot be partitioned into a unique set of convex components.

In contrast, spherical voids (balls) do not tessellate a part of space, unless we fill the interstices with smaller balls (forming an *Apollonian packing* of balls). However, to really represent the structure of the voids in a given distribution, we demand (in our void-finder) that the balls touch the points of the distribution, while some space remains unfilled by the sequence of voids. Thus, the complement of the voids constitutes a fat fractal. The scaling of voids then is less straightforward and can involve a different dimension (the interior dimension of the voids instead of the box-dimension of the mass distribution). However, spherical voids are usually a good approximation to a partition of the empty space into non-degenerate convex regions. In particular, voids scale with the right exponent in our simulations of random self-similar fractals.

Multifractal mass distributions have a spectrum of dimensions and contain singular mass concentrations of variable strength. Therefore, multifractal voids are more complex, but they can actually be classified in two types, which correspond to the two main behaviours of the void probability function in the limit  $V \rightarrow 0$ . Voids of the first type are like monofractal voids, only present when the void probability function tends to one. In contrast, voids of the second type are formed by mass depletions, typical of multifractals, which are present even when the void probability function vanishes. This type of voids appears, for example, in the adhesion model and involves complex geometrical notions. Our classification of voids provides an interpretation of Mandelbrot's lacunarity concept: either type of voids characterizes lacunar or non-lacunar fractals, respectively.

We have illustrated the difference between both types of voids with a deterministic multifractal foam: the Cantor-Sierpinski carpet. The "cosmic web" can be modelled as a random multifractal foam. However, the results of simulations of cold dark matter dynamics are consistent with the presence of the second type of voids only.

Multifractal geometry is complex and not intuitive. Notwithstanding, a coarse-grained mass distribution and, therefore, its coarse-grained voids are sufficient to describe finite



multifractal samples. Both types of multifractal voids mix under coarse graining, becoming excursion sets. In nonlinear (non-Gaussian) fields, the excursion set that defines voids occupies most of the volume but contains little mass. In particular, in the lognormal model, that excursion set is dominated by a percolating void.

After coarse graining, connected multifractal voids still have complicated structures. It is convenient to partition them into simpler regions, for example, convex regions, like we do in cut-out sets. In particular, spherical voids (balls) are adequate for finite multifractal samples. We have studied the distribution of spherical voids in samples of simulated multifractals supported in their whole regions of definition (with voids of the second type only). The log-log plots of the rank-orderings of void sizes are similar to those of Poisson distributions, but the sizes of small voids do not decrease as sharply as in the latter. The voids in distributions of uniform halos are more relevant for the dark matter distribution. The sizes of these voids decrease quite smoothly, without actually scaling.

Regarding voids in the galaxy distribution, we employ a multifractal model of galaxy bias, which we propose as a multifractal version of the “peak theory” of Gaussian fields. It has a free parameter, the halo mass threshold for “wall galaxies”. It is natural to choose a high threshold. Assuming that this threshold is higher than the threshold for galaxy formation in halos, there are galaxies in the voids (“field galaxies” or “void galaxies”). Otherwise, voids do not contain galaxies. Nevertheless, voids defined as excursion sets or spherical voids defined by galaxy samples contain mini-halos with a substantial amount of dark matter.

*Acknowledgements.* I thank Rien van de Weygaert and the other organizers of the Royal Academy Colloquium “Cosmic Voids” in Amsterdam, Dec. 2006, for the invitation to participate in it, where the idea for this work arose. I also thank Anton Tikhonov for sending me his 2dF VLS data and for correspondence, Fernando Barbero for calculating the asymptotic expansion in Eq. (8), and Claude Tricot for sending me some references.

## References

- Aurenhammer F. and Klein R., 2000, *Voronoi diagrams*, in J. Sack, G. Urrutia (eds.), *Handbook of Computational Geometry*, 201–290 (Elsevier Science Publishing)
- Balian R. & Schaeffer R., 1988, *ApJ*, 335, L43
- Balian R. & Schaeffer R., 1989, *A&A*, 220, 1–29
- Bardeen J.M., Bond J.R., Kaiser N. and Szalay A.S., 1986, *ApJ* 304, 15–61
- Betancort-Rijo J., 1990, *MNRAS*, 246, 608–615
- Coles P. and Jones B.J., 1991, *MNRAS*, 248, 1–13
- Cooray A. & Sheth R., 2002, *Phys. Rep.* 372, 1
- Einasto J., Einasto M. and Gramann M., 1989, *MNRAS*, 238, 155–177
- El-Ad H. and Piran T., 1997, *ApJ* 491, 421
- Falconer K., 1997, *Techniques in Fractal Geometry* (John Wiley & Sons, Chichester, UK)
- Franz W., 1965, *General topology* (Ungar, NY)
- Gabrielli A., Sylos Labini F., Joyce M. and Pietronero L., 2005, *Statistical Physics for Cosmic Structures* (Springer, Berlin)
- Gaité, J., 2005-A, *Europhysics Letters* 71, 332–338
- Gaité, J., 2005-B, *Eur. Phys. Jour. B*, 47, 93
- Gaité, J., 2006, *Physica D* 223, 248
- Gaité J., 2007, *ApJ*, 658, 11–24
- Gaité J., Domínguez A. and Pérez-Mercader J., 1999, *ApJ*, 522, L5
- Gaité, J. and Manrubia S. C., 2002, *MNRAS*, 335, 977
- Gottlöber, S., Lokas, E.L., Klypin, A. & Hoffman, Y., 2003, *MNRAS*, 344, 715
- Grebowi C., McDonald S.W., Ott E. and Yorke J.A., 1985, *Physics Letters A*, 110, 1–4
- Harte D., 2001, *Multifractals: theory and applications* (Chapman & Hall, Boca Raton)
- Icke V., 1984, *MNRAS*, 206, 1 P
- Icke V. and van de Weygaert R., 1987, *A&A*, 184, 16–32
- Jones B.J., Coles P. and Martínez V., 1992, *MNRAS*, 259, 146
- Jones B.J., Martínez V., Saar E. and Einasto J., 1988, *ApJ*, 332, L1
- Jones B. J., Martínez V. J., Saar E. and Trimble V., 2004, *Rev. Mod. Phys.* 76, 1211
- Kaiser N., 1984, *ApJ*, 284, L9
- Mandelbrot B.B., 1983, *The fractal geometry of nature* (rev. ed. of: *Fractals*, 1977) (W.H. Freeman and Company, NY)
- Martínez, V.J., Jones, B.J., Domínguez-Tenreiro, R. & van de Weygaert, R., 1990, *ApJ*, 357, 50
- Mekjian, A.Z., 2007, *ApJ*, 655, 1–10
- Otto S., Politzer H.D., Preskill J.P. and Wise M.B., 1986, *ApJ*, 304, 62–74
- Peacock J.A. and Smith R.E., 2000, *MNRAS*, 318, 1144–1156
- Peebles, P.J.E., 1980, *The large-scale structure of the universe* (Princeton U. Press, Princeton, NJ)
- Peebles P.J.E., 2001, *ApJ*, 557, 495–504
- Pietronero L., 1987, *Physica A* 144, 257–284
- Politzer H.D. and Preskill J.P., 1986, *Physical Review Letters*, 56, 99–102
- Shandarin S.F., Sheth J.V. and Sahni V., 2004, *MNRAS*, 353, 162
- She Z., Aurell E. and Frisch U., 1992, *Commun. Math. Phys.*, 148, 623
- Sheth, R.K. & van de Weygaert, R., 2004, *MNRAS*, 350, 517
- Sylos Labini F., Montuori M. and Pietronero L., 1998, *Phys. Rept.*, 293, 61
- Tikhonov A., 2006, *Astron. Lett.*, 32, 727
- Tikhonov A., 2007, *Voids in the SDSS Galaxy Survey*, preprint [arXiv:0707.4283](https://arxiv.org/abs/0707.4283)
- Tikhonov A.V. and Karachentsev I.D., 2006, *ApJ.*, 653, 969
- Tricot C., 1986, *Physics Letters A*, 114, 430
- Tricot C., 1989, *Constr. Approx.*, 5, 117–136
- van de Weygaert R., 2002, *Froth Across the Universe, Dynamics and the Stochastic Geometry of the Cosmic Foam*, in: *Modern Theoretical and Observational Cosmology*, M. Plionis and S. Cotsakis (eds.) Vol. 276, 119 (Kluwer, Dordrecht)
- Vergassola M., Dubrulle B., Frisch U. & Noullez A., 1994, *A&A* 289
- White S.D.M., 1979, *MNRAS*, 186, 145–154
- Zehavi I., et al, 2005, *ApJ*, 630, 1